

Viscoelastic Characterization of Polymers Using Instrumented Indentation – I. Quasi-static Testing

M. R. VanLandingham^{†,a,b} N.-K. Chang^c, C. C. White^b, and S.-H. Chang^c

^b*National Institute of Standards and Technology
Gaithersburg, MD 20899-8615*

^c*Department of Mechanical Engineering, National Taiwan University
Taipei, Taiwan*

[†] Current address: *Army Research Laboratory, Aberdeen Proving Ground, MD 21005*

^aAddress all correspondence to this author; email: mvanlandingham@arl.army.mil

Abstract

The use of instrumented indentation to characterize the mechanical response of polymeric materials was studied. A model based on contact between a rigid probe and a linear viscoelastic material was used to calculate values for creep compliance and stress relaxation modulus for two crosslinking polymeric materials, an epoxy and poly(dimethyl siloxane) or PDMS. The use of a rounded conical tip and sharp pyramidal tips produced linear and nonlinear responses from these two polymers depending on tip shape and load level. Results from bulk rheometry studies were used for comparison to the indentation creep and stress relaxation results.

I. INTRODUCTION

Instrumented indentation is increasingly being used to probe the mechanical response of polymeric and biological materials. These types of materials behave in a viscoelastic fashion, i.e., they display mechanical properties between those of an elastic solid and a viscous fluid. The mechanical behavior is thus dependent on the test conditions, including the amount of strain, the strain rate, and the temperature. Often in instrumented indentation, however, properties are measured using loading histories developed for elastic and elasto-plastic materials, the properties of which are not particularly time dependent. Further, analysis of the indentation response is typically based on elasticity theory. In studies in which attempts have been made to characterize viscoelastic behavior [1, 2], limiting and sometimes invalid assumptions have been made, and linear viscoelasticity has been applied despite the intense strains local to the indenter tip that would appear to violate the linear viscoelasticity premise of infinitesimal strains [3].

For conical or pyramidal tip geometry, a nominal indentation strain is related to the characteristic included angle or angles of the tip. For a paraboloidal tip, indentation strain is related to the ratio of the contact radius, r , to the tip radius, R , and r is related to the displacement, h [4-6]. For any tip geometry, the indentation strain rate can be calculated from the ratio \dot{h}/h , where \dot{h} is the rate of change of h with time, t , or $\dot{h} = dh/dt$. The mean stress or hardness, H , is the ratio of load, P , to contact area, A , where A is in general related to displacement by the tip geometry. Only in the case of a flat punch, where A is constant with h , is H a function of load only. For Vickers and Berkovich pyramidal indenters, which ideally have the same area function, $A(h)$, analyses

attributed to Tabor [4] yield an estimated representative strain for these self-similar tips of approximately 8 %. However, Chaudhri [7] estimated that representative strain ranges from 25 % to 36 % for a Vickers indentation of polycrystalline copper using FET, and finite element analysis has been used to estimate strains local to a Berkovich indenter to be in excess of 100 % with a significant volume of material subjected to at least 15 % strain [8]. As discussed by Dao et al. [8], values for representative indentation strain will depend on the relationships between indentation parameters and mechanical properties upon which its definition is based. Thus, for indentation of polymeric materials, representative strain maybe different from that defined previously in other studies, and it may even differ between quasi-static and dynamic indentation testing.

To better assess the indentation response of polymeric materials, mathematical analyses of quasi-static contact between a rigid indenter and a linear viscoelastic solid [9-14] can be used. These analyses are based upon the development of an appropriate boundary-value problem that satisfies the equations of equilibrium:

$$\frac{\partial \sigma_{ij}}{\partial x_{ij}} = 0 \quad (1)$$

In this equation, σ_{ij} is stress and x_{ij} are Cartesian coordinates [10, 11], and the stress-strain relations for linear, isotropic viscoelasticity are given by [12]:

$$e_{ij}(t) = \int_0^t J(t-\tau) \frac{\partial}{\partial \tau} s_{ij}(\tau) d\tau \quad s_{ij}(t) = \int_0^t G(t-\tau) \frac{\partial}{\partial \tau} e_{ij}(\tau) d\tau \quad (2)$$

$$\varepsilon_{ij}(t) = \int_0^t B(t-\tau) \frac{\partial}{\partial \tau} \sigma_{ij}(\tau) d\tau \quad \sigma_{ij}(t) = \int_0^t K(t-\tau) \frac{\partial}{\partial \tau} \varepsilon_{ij}(\tau) d\tau \quad (3)$$

$B(t)$ and $K(t)$ are the dilatational creep and relaxation functions, respectively, relating the stress and strain invariants, σ_{ii} and ε_{ii} , and t is time. $J(t)$ and $G(t)$ are the shear creep and relaxation functions, respectively, relating the deviatoric stress tensor, s_{ij} , and the deviatoric strain tensor e_{ij} , defined respectively as:

$$s_{ij} = \sigma_{ij} - \frac{1}{3} \sigma_{kk} \delta_{ij} \quad e_{ij} = \varepsilon_{ij} - \frac{1}{3} \varepsilon_{kk} \delta_{ij} \quad (4)$$

Here, δ is the Kronecker delta ($\delta = 1$ for $i = j$, $\delta = 0$ for $i \neq j$). Strain is given in terms of displacements, u , by:

$$\varepsilon_{ij} = \frac{1}{2} \left(\frac{\partial u_i}{\partial x_j} + \frac{\partial u_j}{\partial x_i} \right) \quad (5)$$

The previous expressions relating stress and strain are formulated in terms of integral operators associated with the hereditary function, such that relaxation times are given by a continuous spectrum. Alternatively, these expressions can be restated in terms of differential operators using a viscoelastic model of springs and dashpots, corresponding to a discrete spectrum of

relaxation times, or using other equivalent ways of expressing linear viscoelastic behavior, including direct measurements [9, 10, 12]. One such formulation is the following linear viscoelastic stress-strain relation [11, 13]:

$$\sigma_{ij} = \int_{0^-}^t \left[2G(t-\tau) \frac{\partial \varepsilon_{ij}(\tau)}{\partial \tau} + \delta_{ij} E(t-\tau) \frac{\partial \varepsilon_{kk}(\tau)}{\partial \tau} \right] d\tau \quad (6)$$

$E(t)$ and $G(t)$ are the relaxation moduli in extension and shear, respectively, and the lower limit of 0^- is used in case of a jump in stresses and strains at $t = 0$. For homogeneous, isotropic, elastic materials, E and G are related by:

$$G = \frac{E}{2(1+\nu)} \quad (7)$$

The bulk modulus, K , is related to E by:

$$K = \frac{E}{3(1-2\nu)} \quad (8)$$

In these equations, ν is the Poisson's ratio. These equations hold for a viscoelastic solid only at equilibrium. Also, for viscoelastic materials, the shear, bulk, and extensional creep compliances, $J(t)$, $B(t)$, and $D(t)$, respectively, are not simple inverse functions of their respective relaxation moduli, $G(t)$, $K(t)$, and $E(t)$, as they are for elastic materials, and ν is, in general, a function of time [3], although it is often taken to be constant for simplicity.

Viscoelastic solutions to boundary value problems can often be solved by applying the Laplace transform to remove the variable, t , from the system of equations. This approach yields an elastic problem in the transformed variables. Using the elastic solution to the transformed problem, a viscoelastic solution is achieved by replacing the elastic constants with the appropriate viscoelastic operators and then performing the inverse Laplace transform. In the case of the given contact problem, however, the boundary conditions are normally given from compatibility between displacements and stresses with the prescribed surface displacements and surface tractions, respectively, and these conditions are a function of time [9-11]. Therefore, in general, the transform approach is not applicable, although a solution by Lee and Radok of this type for an incompressible material ($\nu = 0.5$) has been shown to be valid for monotonically increasing contact radius [10]. A slightly different approach by Ting yields solutions for increasing and decreasing contact radius values that are applicable to compressible materials [11].

For the case of indentation creep, in which a constant load P_0 is applied at $t = 0$ and held, both the Lee and Radok model and the Ting model give the same functional relationship between creep compliance, $J(t)$, P_0 , contact area, $A(t) = \pi r^2(t)$, and penetration depth, $h(t)$, for a paraboloidal indenter of radius R :

$$J(t) = \alpha \frac{h(t)\sqrt{A(t)}}{P_0} \quad (9)$$

In this equation, α is a constant of proportionality with a nominal value of $8/(3\sqrt{\pi})$. Similarly, for relaxation under conditions in which a constant penetration depth h_0 is applied at $t = 0$ and held using a spherical indenter of radius R , both models give the following relationship between the relaxation modulus, $G(t)$, h_0 , the corresponding contact area, A_0 , and the load, $P(t)$:

$$G(t) = \alpha' \frac{P(t)}{h_0 \sqrt{A_0}} \quad (10)$$

Again, α' is a constant of proportionality with a nominal value of $(3\sqrt{\pi})/8$. Additionally, the Ting model yields equations for constant-load indentation creep and constant-depth stress relaxation for conical tips:

$$J(t) = \beta \frac{A(t) \tan \theta}{P_0} \quad (11)$$

$$G(t) = \beta' \frac{P(t)}{A_0 \tan \theta} \quad (12)$$

In these equations, θ is the cone semi-apical angle, and β and β' are constants of proportionality nominally equal to 1.0. Relationships similar to Eq. (11) and Eq. (12) – only the constants of proportionality differ by a factor of $1/[2 \cdot (1 - \nu^2)]$ – were recently derived for pyramidal indenters [6] directly from Hook's law by assuming that a representative stress was given by P/A and a representative strain is given by $(\tan \theta) \cdot (dh/h)$. Note that an additional factor is sometimes applied to indentation analysis that is related to non-circular contact areas of pyramidal tips [8].

Because of the intense stresses and strains local to the tip-sample contact, whether or not linear viscoelasticity is obeyed during instrumented indentation measurements is difficult to ascertain. Further, because the mechanical behavior of polymeric and biological materials is dependent on the test conditions, including the amount of strain and the strain rate, understanding the viscoelastic behavior is important for analyzing indentation data for these types of materials. One test of linear viscoelasticity is the lack of dependence of the creep compliance (or stress relaxation modulus) on the magnitude of the stress (or strain). Equation (9) through Equation (12) present an opportunity to determine for paraboloidal and conical (and presumably for pyramidal) indentation probes whether linear viscoelasticity is obeyed under particular test conditions. Additionally, these equations provide a means for measuring viscoelastic behavior using instrumented indentation that can be compared to traditional solid rheological measurements.

In this paper, analyses based on contact between a rigid indenter and a linear viscoelastic material are used to determine under what conditions, if any, can instrumented indentation be used to measure linear viscoelastic behavior. Three different polymers are characterized using

traditional solid rheology and using constant-load indentation creep and constant-depth stress relaxation measurements with different indentation probe geometries. For the indentation measurements, checks of linear viscoelasticity are performed by studying the dependence of creep compliance on indentation load. The resulting measurements of creep compliance and relaxation modulus are compared to traditional solid rheology measurements. In the following sections, the experimental details are presented, followed by results and discussion and then conclusions.

II. EXPERIMENTAL¹

A. Materials

Materials used in this study included an amine-cured epoxy and poly(dimethyl siloxane) (PDMS). Epoxy films approximately 190 μm in thickness were cast onto silicon wafers in a CO_2 -free and H_2O -free glove box using a drawdown technique. Highly pure diglycidyl ether of bisphenol A with a mass per epoxy equivalent of 172 g and 1,3-bis(aminomethyl)-cyclohexane were mixed at the stoichiometric ratio. All samples were cured at room temperature for 48 h, followed by post-curing at 130 $^\circ\text{C}$ for 2 h. The films were then removed from the silicon substrates by immersion in warm water followed by peeling with tweezers. The glass transition temperature, T_g , of the cured films were (123 ± 2) $^\circ\text{C}$, as estimated using dynamic mechanical analysis. The Dow Corning Corporation generously provided PDMS samples, with an approximate thickness of 3.2 mm.

B. Solid rheology measurements

Stress relaxation measurements were made in torsion on PDMS samples using an Advanced Rheometric Expansion System or ARES (Rheometrics Scientific, Inc.) and in tension on both the PDMS and epoxy samples using a Rheological Solids Analyzer or RSA II (Rheometrics Scientific, Inc.). Both instruments are displacement-controlled systems capable of performing stress relaxation tests. The amount of strain is determined from the applied displacement or torsional angle and the sample geometry and a load transducer measures the resulting force. Instrumental capabilities limited the amount of strain applied on PDMS samples in the ARES to 0.08 (8%) and in the RSA II to 0.01 (1%).

For a traditional creep test, creep compliance, $J(t)$, is defined as

$$J(t) = \frac{\varepsilon(t)}{\sigma_0} \quad (13)$$

Normally, a constant load is applied and the displacement is monitored with time and converted to constant stress, σ_0 , and strain, $\varepsilon(t)$, respectively, using the original dimensions of the sample, which are measured prior to testing. Similarly, the stress relaxation modulus, $E(t)$, is defined as

¹ Certain commercial instruments and materials are identified in this paper to adequately describe the experimental procedure. In no case does such identification imply recommendation or endorsement by the National Institute of Standards and Technology, nor does it imply that the instruments or materials are necessarily the best available for the purpose.

$$E(t) = \frac{\sigma(t)}{\varepsilon_0} \quad (14)$$

Stress, $\sigma(t)$, in this case is a function of time during the application of a constant displacement, which is converted to a constant strain, ε_0 . Creep compliance and stress relaxation modulus are related by the following two equivalent equations:

$$\int_0^t E(t-\tau)J(\tau)d\tau = t \quad (15a)$$

$$\int_0^t J(t-\tau)E(\tau)d\tau = t \quad (15b)$$

Additionally, $E(0)J(0) = 1$ and $E(\infty)J(\infty) = 1$. Equation (7) was used to convert measurements of stress relaxation modulus in shear, $G(t)$, to that in tension, $E(t)$, assuming values of ν of 0.3 for epoxy and 0.5 for PDMS.

C. Instrumented indentation measurements

Instrumented indentation was performed using a NanoIndenter XP and a NanoIndenter DCM (MTS Systems, Inc.). The XP system, in general, was used for applied loads from 100 mN down to 0.2 mN, while the DCM system was used for applied loads from 10 mN down to 0.01 mN. For measurements made with the XP system, two different probe tip shapes were used, including a Berkovich pyramid and a rounded 90° cone with a tip radius of approximately 10 μm , respectively. Only a Berkovich tip was available for testing with the DCM system. Tip shape has been measured for these probes using indentation of reference samples and by directly imaging the probes with an atomic force microscope (AFM), as detailed elsewhere [15].

Indentation creep response was measured using step loading to a prescribed load, P_0 , which was then held for 100 s. For a given test, P_0 was reached in less than 0.5 s and was maintained within $\pm 2 \mu\text{N}$ for the XP system and $\pm 1 \mu\text{N}$ for the DCM system. After this near-step loading, however, the dynamic oscillation superposed over the constant load required time to stabilize before measurements of contact area were considered to be accurate. This time laps was approximately (10 to 12) s for the XP system and (4 to 5) s for the DCM system. The constant load was then held for approximately 100 s, at which point the creep rates for the two polymers became of the same order as the thermal drift of the system (approximately $\pm 0.2 \text{ nm/s}$), which was estimated by performing the same constant load tests on fused silica before and after each set of tests on a polymer sample. Because the system thermal drift could be positive or negative, no attempt was made to remove the system drift from the creep measurements. For a set of 5 tests at the same nominal load, the difference between the lowest and highest values of P_0 was less than 3 μN for both systems, regardless of the magnitude of the prescribed load. Examples of system performance are shown in Fig. 1 for the XP system and Fig. 2 for the DCM system. Creep compliance was calculated using Eq. (9) or Eq. (11) depending on the tip geometry. Nominal values of the proportionality constants were used in all such calculations. Poisson's ratio was assumed to be constant for all calculations and equal to 0.3 for the epoxy and 0.5 for the PDMS.

Indentation relaxation response was measured using a step displacement to a prescribed depth, h_0 . This depth was then held for 100 s. For a given test, h_0 was reached in approximately 6 s, followed by a period of roughly (6 to 8) s during which the system feedback attempts to control the displacement at the prescribed constant value. A slight overshoot of approximately (5 to 10) % of h_0 was observed for the XP system and (1 to 3) % of h_0 for the DCM system. After the initial overshoot, displacement was maintained within \pm (1-2) nm for both the XP and DCM systems, except for very large displacements with the XP system, for which displacement variations were as much as \pm 5 nm for a nominal displacement of 4000 nm (see Fig. 3a). For a set of 10 tests at the same nominal depth, the difference between the lowest and highest values of h_0 was less than 5 nm for both systems for target depths of 1500 nm or less, and 10 nm for target depths greater than 1500 nm. However, repeatability of the load values was much better for the DCM system compared to the XP system. Examples of system performance are shown in Fig. 3 for the XP system and Fig. 4 for the DCM system. Again, the length of the relaxation tests was 100 s to minimize uncertainty due to system thermal drift. Relaxation modulus was calculated using Eq. (10) or Eq. (12) depending on the tip geometry. Nominal values of the proportionality constants were used in all such calculations. Poisson's ratio was assumed to be constant for all calculations and equal to 0.3 for the epoxy and 0.5 for the PDMS.

III. RESULTS AND DISCUSSION

An example of indentation creep compliance determined for an epoxy sample using a rounded conical tip (manufacturer-determined tip radius of 10 μm) is shown in Fig. 5. The creep compliance is clearly dependent on indentation loads between 0.2 mN and 20 mN, which is an indication of nonlinear behavior. Creep compliance was also observed to be a function of load for the epoxy sample using Berkovich indentation tips for both the XP head (Fig. 6) and the DCM head (Fig. 7). The compliance values for the two Berkovich tips were similar for similar applied load levels with differences likely due to slight differences in tip geometry, leading to differences in stresses and strains. Qualitatively, the data appears to be consistent with behavior expected of a glassy epoxy polymer [16] – compliance values are on the order of 10^{-9} Pa and trend higher with increasing creep time and increasing load. Additionally, the variation of compliance with time appears to have similar curvature for each of the load levels studied using the rounded cone and for the higher load levels using the Berkovich tips, suggesting separability of the time-dependent behavior from the stress-dependent behavior. The differences in slope at the lower indentation creep loads for the Berkovich tips (Figs. 6 and 7) could have resulted from uncertainties in tip shape related to indentation depths less than 100 nm.

Indentation creep compliance results for PDMS using a Berkovich tip and the DCM system are shown in Fig. 8. Again, the data appears to be consistent with expected behavior [3] – compliance values are on the order of 10^{-6} Pa and trend slightly higher with increasing creep time but decrease with increasing load. Additionally, although the data scatter was significant, the compliance values for an intermediate load range between 100 μN and 2 mN appear to be similar, potentially indicating a region of linear behavior. This behavior will be discussed further with regard to the stress relaxation results.

As detailed in the Experimental section, a dynamic oscillation was superposed over the creep load using a controlled displacement amplitude of approximately 5 nm and a frequency of 45 Hz for both the XP and DCM systems. While the harmonic displacement was generally small

relative to the quasi-static displacements, high frequency heating was a possibility that would potentially alter the measured response compared to an indentation creep test without this dynamic component. In Fig. 9, displacement response to several creep loads are shown as a function of time for both epoxy and PDMS. In both cases, the evolution of displacement with time was identical within experimental uncertainty for measurements made with and without the dynamic oscillation component.

Results of stress relaxation testing are presented in Fig. 10 and Fig. 11 for epoxy and PDMS, respectively, including indentation and rheometry data. For the data measured with the RSA II rheometer in tension on the epoxy material, the stress relaxation modulus values were similar for strain levels of 0.01 % and 0.1 %. The application of a 1 % strain, however, resulted in significantly lower relaxation modulus values and perhaps a slight increase in curvature compared to the two lower strain levels, which is indicative of nonlinear behavior. Similar behavior was observed for the stress relaxation modulus values measured using indentation with a Berkovich tip. Increases in the constant displacement applied resulted in lower relaxation modulus values. Although changes in curvature were difficult to observe due to the data scatter, the time-dependence, which is relatively small for this glassy epoxy at room temperature, measured with indentation is similar to that measured with rheometry.

For the PDMS material, nonlinear behavior was observed in the rheometry measurements in both tension and torsion, as the stress relaxation modulus decreased with increasing strain levels. Additionally, the curvature decreases with increasing strain such that the PDMS exhibits little time dependence at higher strain levels. The indentation relaxation modulus values, however, are independent of penetration depth for depths from 1000 nm up to 5000 nm within the data scatter. For penetration depths of 10 μm and 15 μm , the relaxation modulus values are again similar but slight higher compared to those for the three smaller penetration depths. However, the tip shape was not characterized for distances greater than 3000 nm from the tip apex, so uncertainty in the contact area at these depths could be quite large. PDMS materials often behave in a nonlinear elastic fashion with little time dependence. Further, at high strains, for example about 10 % strain, PDMS behavior becomes more linear. Both the rheometry data and the indentation data appear to be consistent with these statements, showing similar but small amounts of time dependence with the presumably much larger strain indentation measurements showing essentially linear behavior.

In Fig. 12, effective strains are calculated for the Berkovich and rounded conical tip shapes used with the XP system. Calculations of effective strains were based on analyses due to Tabor [4] assuming ideal plastic behavior, and are thus for illustrative purposes only. The following two equations were used for ideal paraboloidal and conical tip geometries, respectively:

$$\bar{\epsilon} = 0.2r / R \quad (16)$$

$$\bar{\epsilon} = 0.03 \tan \theta \quad (17)$$

For the Berkovich tip, an effective conical angle, θ , was determined to be approximately 70.45°. For the rounded cone, an effective radius, R_{eff} , which was determined from tip shape analysis to be a function of the distance from the apex, was used [15]. In this plot, the relative effective strain is lower for the rounded conical tip compared to the Berkovich tip for all creep tests on

epoxy except the two highest loads, 10 mN and 20 mN. In Fig. 13, data from Fig. 5 and Fig. 6 are combined to show that the corresponding relative creep compliance values are lower for the rounded conical tip, except for the two highest loads. Thus, at these two loads, the effective strain levels and the creep compliance values for the rounded conical tip are similar to those for the Berkovich tip. Also, larger variation in creep compliance for the rounded conical tip with load might reflect the larger expected changes in the associated effective strain compared to the Berkovich tip, for which a smaller variation in creep compliance with load was observed, possibly in response to a small variation in effective strain related to deviations in the actual tip geometry from the ideal case plotted in Fig. 12. For the stress relaxation modulus data for epoxy and PDMS (Fig. 10 and Fig. 11, respectively), any potential vertical shifting of the curves as a function of strain level would tend to indicate much larger effective strains in the indentation measurements relative to the rheology measurements. Because the calculations of indentation creep compliance and stress relaxation modulus are based on a linear viscoelastic model and the proportionality constants in Eq. (9) through Eq. (12) are not well known [11], the absolute magnitudes of the indentation data plotted in Figs. 5-8, 10, 11 and 13 are not without significant uncertainty. However, the behavior exhibited appears to be consistent with rheometry measurements and with known bulk rheology of these polymers at the high stress and strain levels expected local to the indentation probe tip.

IV. SUMMARY AND CONCLUSIONS

The use of instrumented indentation to characterize the mechanical response of polymeric materials was studied. A model based on contact between a rigid probe and a linear viscoelastic material was used to calculate values for creep compliance and stress relaxation modulus for epoxy and PDMS materials. The use of sharp pyramidal tips produced nonlinear viscoelastic response from these polymers, while the use of a rounded conical tip produced both linear and nonlinear responses depending on the polymer and the load level. Comparisons to bulk rheometry studies were used for comparison purposes. Unfortunately, the magnitudes of the indentation and rheometric values of creep compliance or stress relaxation modulus are difficult to compare directly. This deficiency is related to the following factors:

- 1) The indentation values were calculated using an analytical model based on linear viscoelastic behavior. However, the majority of the responses measured were nonlinear.
- 2) While the indentation data appeared to reveal behavior with characteristic time-strain or time-stress separability, the data are too limited for any potential application of shift factors based on strain or stress levels, as might be done in a simplified non-linear analysis.
- 3) Often in the analysis of instrumented indentation data, factors are applied to correct for differences in experimental contact conditions compared to model contact conditions. However, these correction factors have been determined for linear elastic and elastoplastic constitutive behavior, and the appropriateness of their use for viscoelastic behavior is unknown.

However, the trends in the indentation data are similar to those in the rheometry data, suggesting that the measurements have sufficient physical similarity. New analyses and measurement

protocols are currently being explored for developing a more complete understanding of the relationships between instrumented indentation data and viscoelastic characterization.

Acknowledgements

The authors gratefully acknowledges fruitful collaborations with John Villarrubia of NIST regarding tip shape determination, Xiaohong Gu of the University of Missouri – Kansas City for epoxy sample preparation, and Vincent Jardret at MTS Systems Corp. for help with test method development. The authors also acknowledge helpful discussions with Sheng Lin-Gibson, Don Hunston of NIST and Greg McKenna of Texas Tech University.

References

1. L. Cheng, X. Xia, W. Yu, L. E. Scriven, and W. W. Gerberich, *J. Poly. Sci. B – Poly. Phys.* 38, 10-22 (2000).
2. K. B. Yoder, S. Ahuja, K. T. Dihn, D. A. Crowson, S. G. Corcoran, L. Cheng, W. W. Gerberich, in: *Fundamentals of Nanoindentation and Nanotribology 522* (Materials Research Society – Proceedings, Pittsburgh, PA, USA 1998), pp. 205.
3. J. D. Ferry, *Viscoelastic Properties of Polymers*, 3rd ed. (John Wiley & Sons, Inc. New York, USA 1980).
4. D. Tabor, *Hardness of Metals*, 3rd ed. (Clarendon Press, Oxford, England 1951).
5. B. J. Briscoe, L. Fiori, and E. Pelillo, *J. Phys. D – Appl. Phys.* 31, 2395-2405 (1998).
6. S. Shimizu, T. Yanagimoto, M. Sakai, *J. Mater. Res.* 14, 4075 (1999).
7. M. M. Chaudhri, *Acta Mater.* 46, 3047 (1998).
8. M. Dao, N. Chollacoop, K. J. Van Vliet, T. A. Venkatesh and S. Suresh, *Acta Mater.* 49, 3899-3918 (2001).
9. E. H. Lee, *Quarterly Appl. Mathematics* 13, 183 (1955).
10. E. H. Lee and J. R. M. Radok, *J. Appl. Mech.* 27, 438 (1960).
11. T. C. T. Ting, *J. Appl. Mech.* 33, 845 (1966).
12. W. H. Yang, *J. Appl. Mech.* 33, 395 (1966).
13. S. C. Hunter, *J. Mech. Phys. Solids* 8, 219 (1960).
14. G. A. C. Graham, *Int. J. Engng. Sci.* 3, 27 (1965).
15. M. R. VanLandingham, R. Camara, and J. S. Villarrubia, *J. Mater. Res.* to be submitted.
16. A. Lee and G. B. McKenna, *Polymer* 31, 423-430 (1990).

Figure Captions

FIG. 1: Examples of system performance for the indentation creep tests are shown for the XP system: (a) 20 mN load, and (b) 200 μ N load. Both examples are for a Berkovich tip indenting epoxy.

FIG. 2: Examples of system performance for the indentation creep tests are shown for the DCM system: (a) 5 mN load, and (b) 10 μ N load. Both examples are for a Berkovich tip indenting epoxy.

FIG. 3: Examples of system performance for the indentation stress relaxation tests are shown for the XP system: (a) 4000 nm displacement, and (b) 500 nm displacement. Both examples are for a Berkovich tip indenting epoxy

FIG. 4: Examples of system performance for the indentation stress relaxation tests are shown for the DCM system: (a) 1500 nm displacement, and (b) 100 nm displacement. Both examples are for a Berkovich tip indenting epoxy

FIG. 5: Log-log plot of creep compliance, $J(t)$, as a function of time, t , for an indentation creep experiment on epoxy using a rounded conical tip (manufacturer-determined tip radius of 10 μ m) and the XP system. Each data point represents an average value from 10 experiments with the error bars representing an estimated standard deviation ($k = 1$). In some cases, the error bars are smaller than the data point symbols.

FIG. 6: Log-log plot of creep compliance, $J(t)$, as a function of time, t , for an indentation creep experiment on epoxy using a Berkovich tip and the XP system. Each data point represents an average value from 10 experiments with the error bars representing an estimated standard deviation ($k = 1$).

FIG. 7: Log-log plot of creep compliance, $J(t)$, as a function of time, t , for an indentation creep experiment on epoxy using a Berkovich tip and the DCM system. Each data point represents an average value from 10 experiments with the error bars representing an estimated standard deviation ($k = 1$).

FIG. 8: Log-log plot of creep compliance, $J(t)$, as a function of time, t , for an indentation creep experiment on PDMS using a Berkovich tip and the DCM system. Each data point represents an average value from 10 experiments with the error bars representing an estimated standard deviation ($k = 1$). Superposed on the plot are rheometry results from both the torsional rheometer and the DMA system.

FIG. 9: Displacement plotted as a function of time for indentation creep tests with and without a superposed 5 nm amplitude dynamic oscillation at 45 Hz for several quasi-static creep load levels: (a) epoxy and (b) PDMS. All data is for the DCM system and a Berkovich tip.

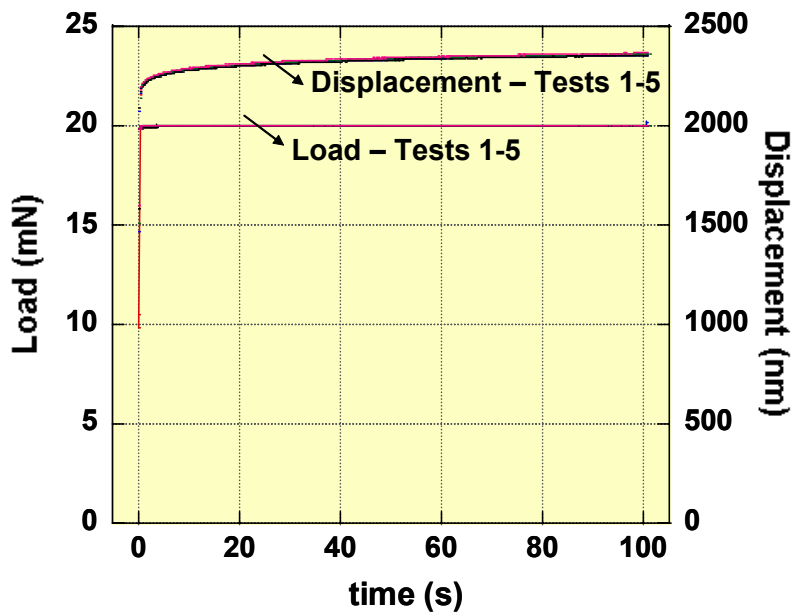
FIG. 10: Log-log plot of stress relaxation modulus, $E(t)$, as a function of time, t , for an indentation relaxation experiment on epoxy using a Berkovich tip and both the XP and DCM systems. Each data point represents an average value from 10 experiments. Superposed on the plot are rheometry results from the RSA II system in tension, for which each data point

represents an average of 3 experiments. For all data shown, the error bars represent an estimated standard deviation ($k = 1$). The percentages in the legend for the tensile rheometry data represent the percent strain applied to the samples.

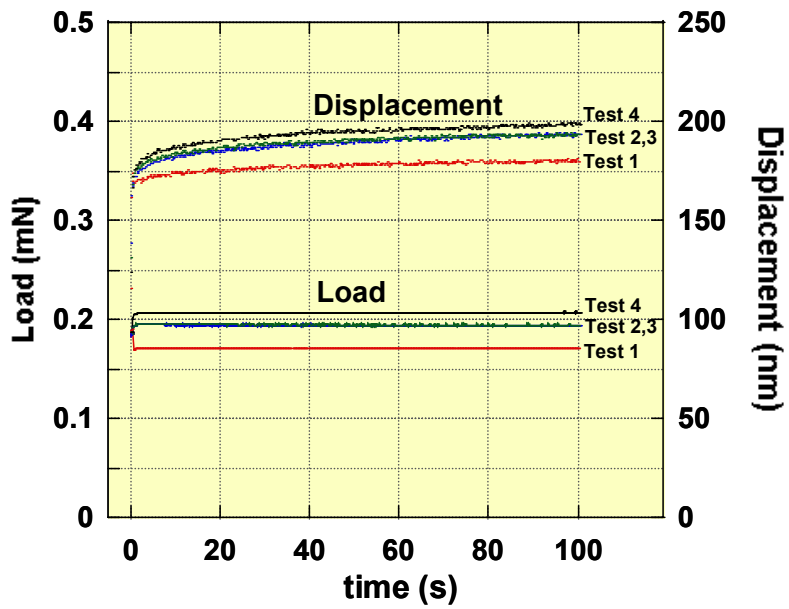
FIG. 11: Log-log plot of stress relaxation modulus, $E(t)$, as a function of time, t , for an indentation relaxation experiment on epoxy using a Berkovich tip and the DCM system. Each data point represents an average value from 10 experiments. Superposed on the plot are rheometry results from both the ARES torsional rheometer and the RSA II system in tension, for which each data point represents an average of 3 experiments. For all data shown, the error bars represent an estimated standard deviation ($k = 1$). The percentages in the legend for the tensile and torsional rheometry data represent the percent strain applied to the samples.

FIG. 12: Plot of effective strain estimates (after Tabor [4]) from various analytical and numerical modeling studies, including predictions of effective strain from tip shape information measured for the Berkovich and rounded conical tips used in this study.

FIG. 13: Log-log plot of creep compliance, $J(t)$, as a function of time, t , comparing the indentation creep data for epoxy from Fig. 5 (rounded conical tip and XP) and Fig. 6 (Berkovich tip and XP). Error bars were removed for clarity.

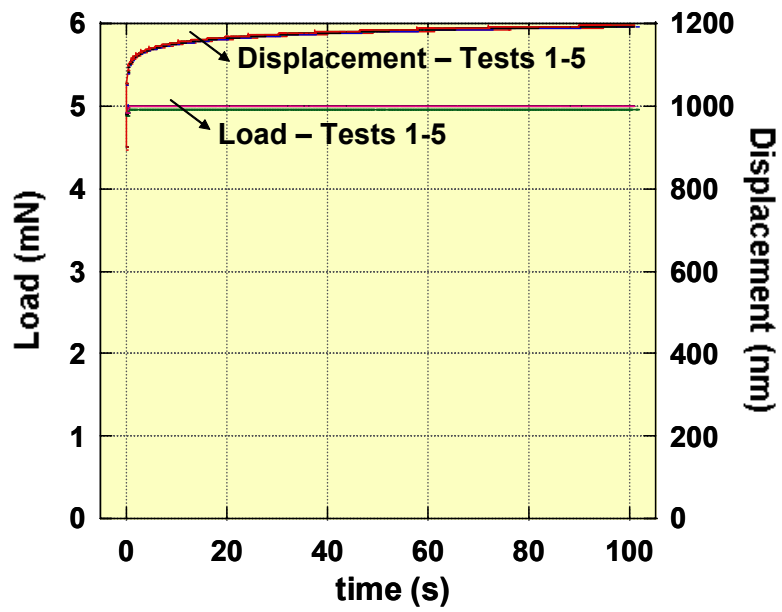


(a)

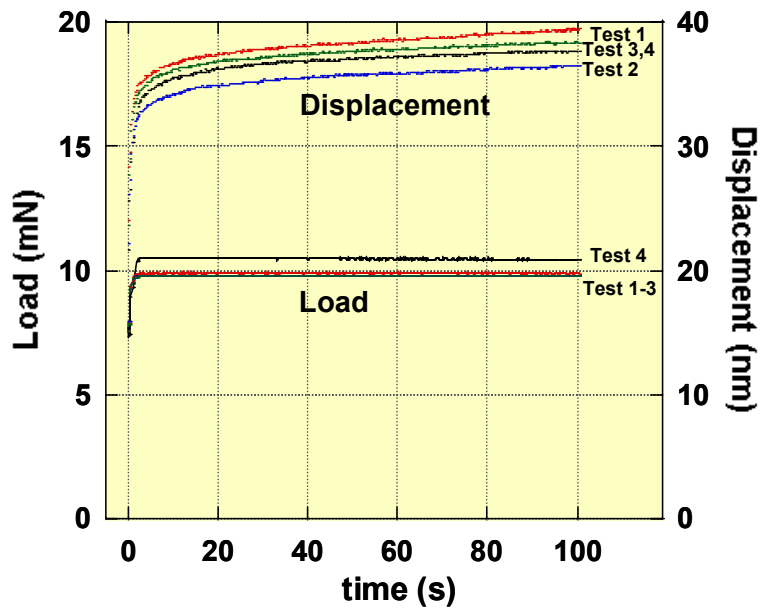


(b)

FIG. 1

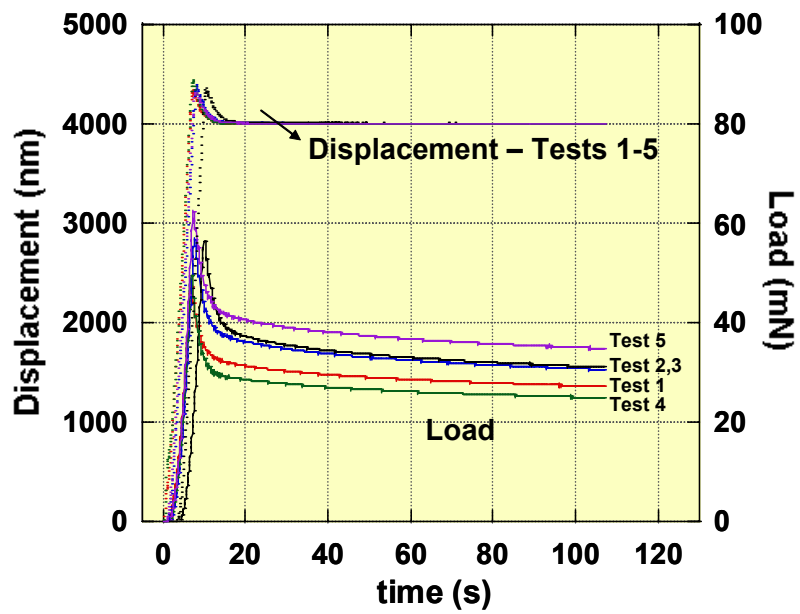


(a)

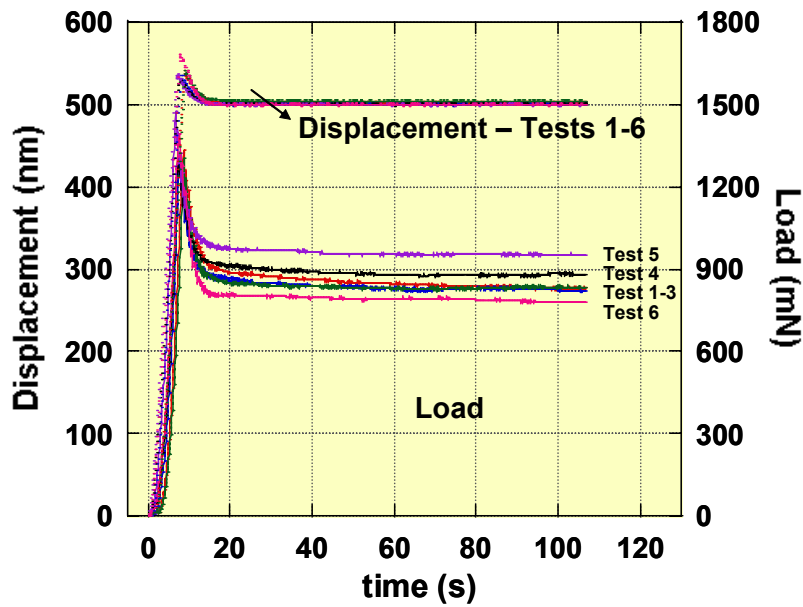


(b)

FIG. 2

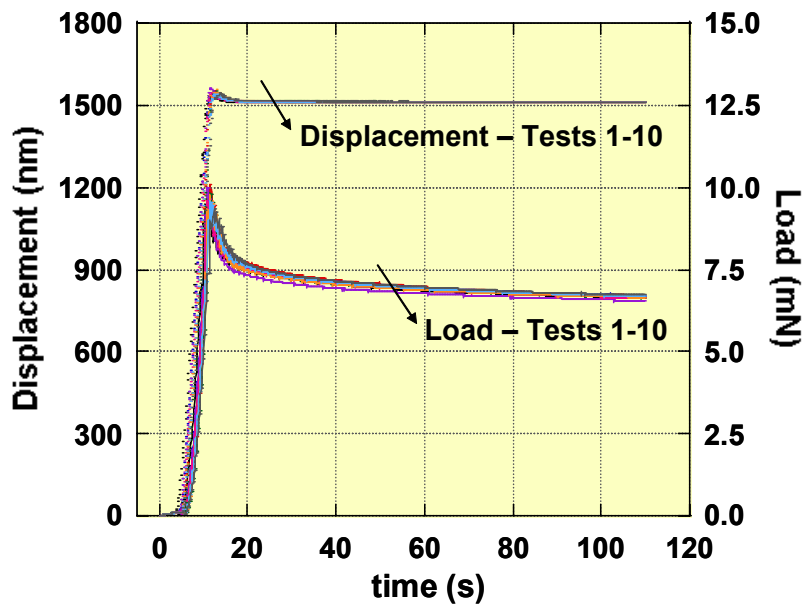


(a)

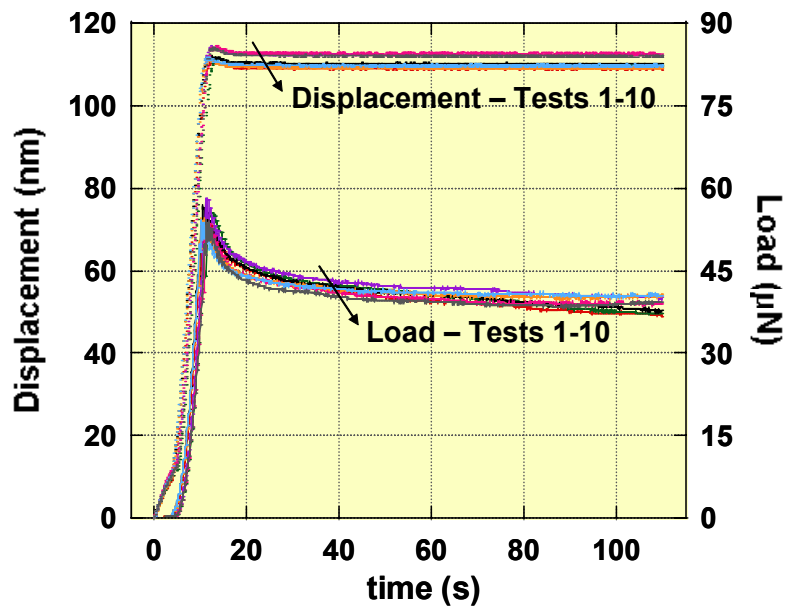


(b)

FIG. 3



(a)



(b)

FIG. 4

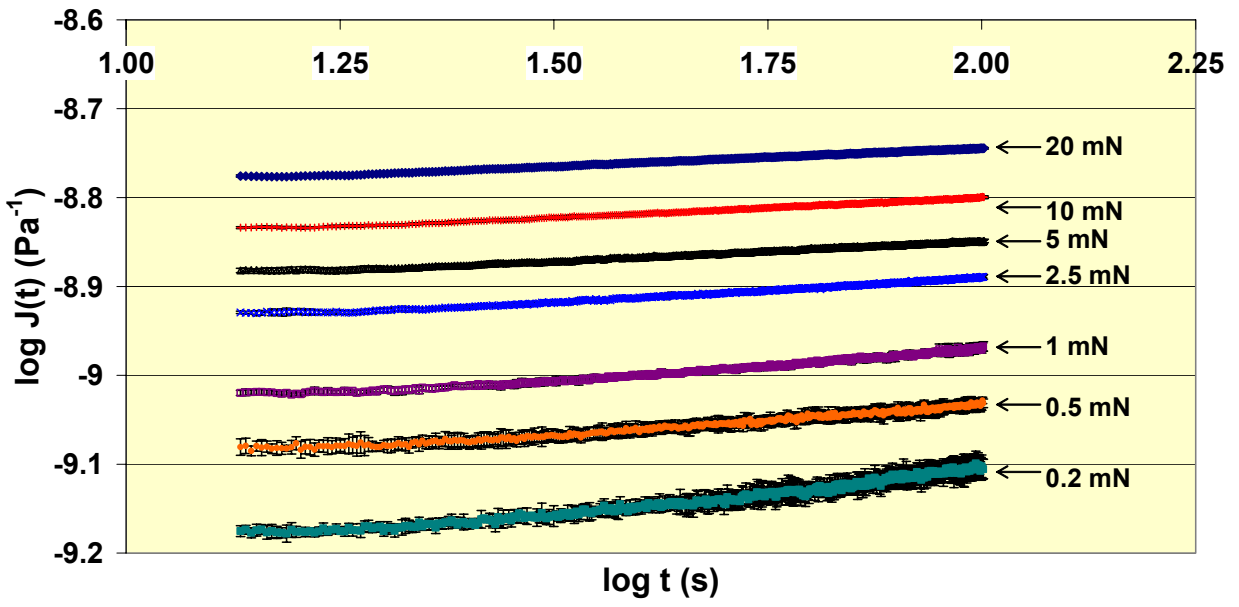


FIG. 5

VanLandingham et al.

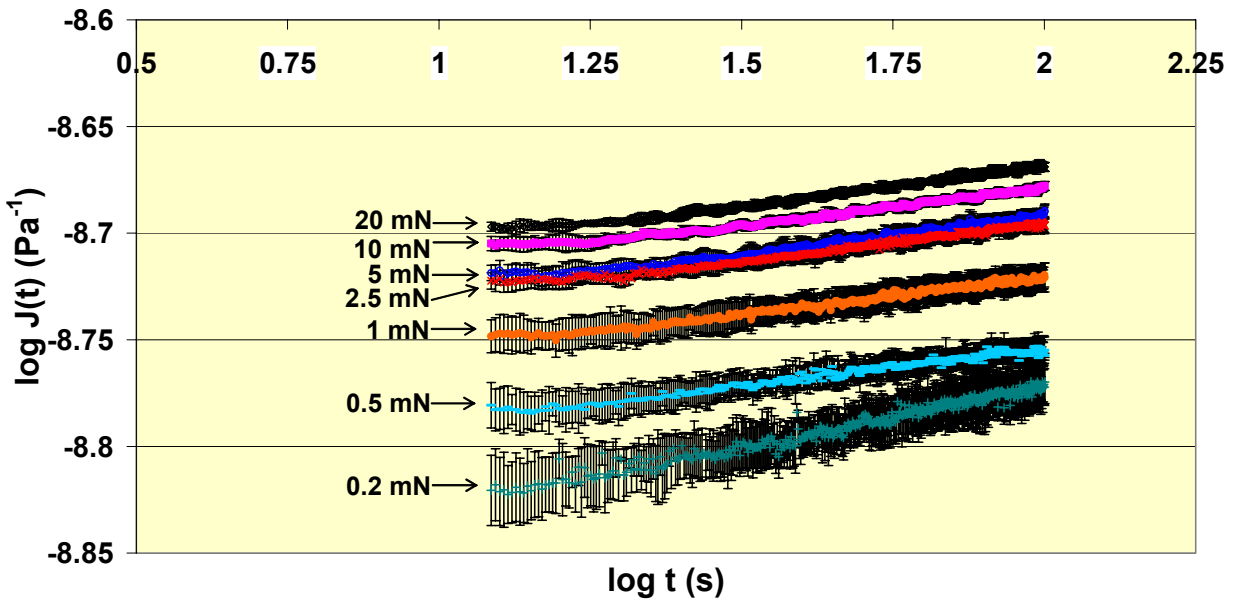


FIG. 6

VanLandingham et al.

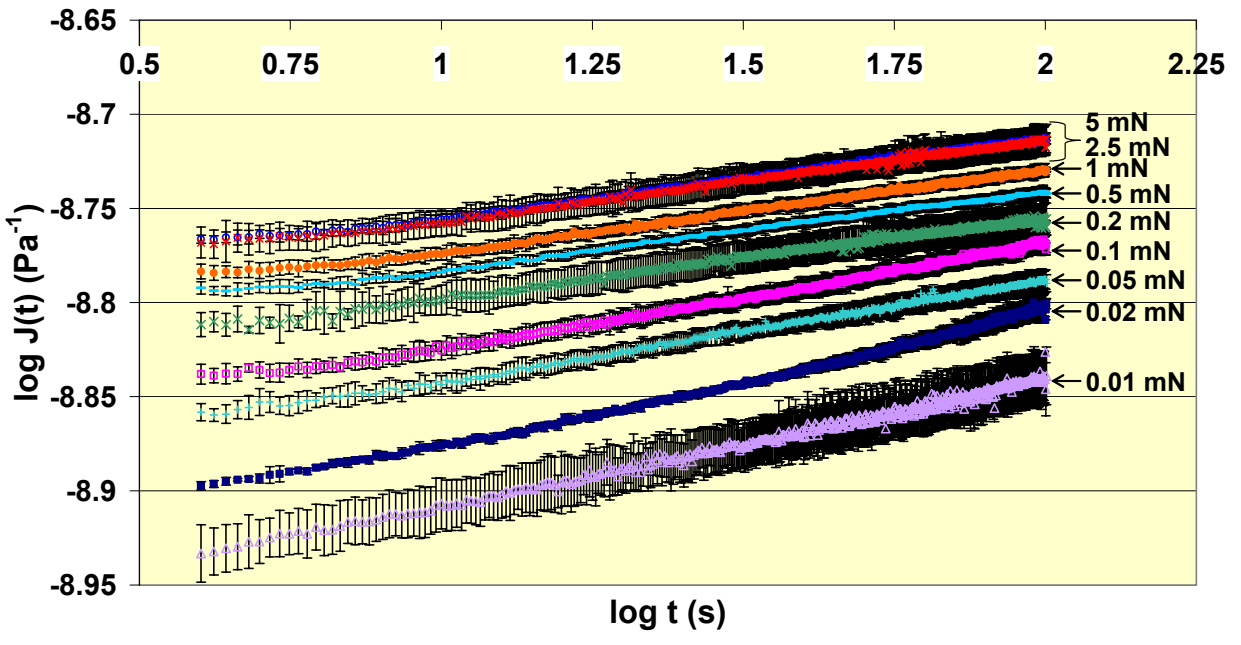


FIG. 7

VanLandingham et al.

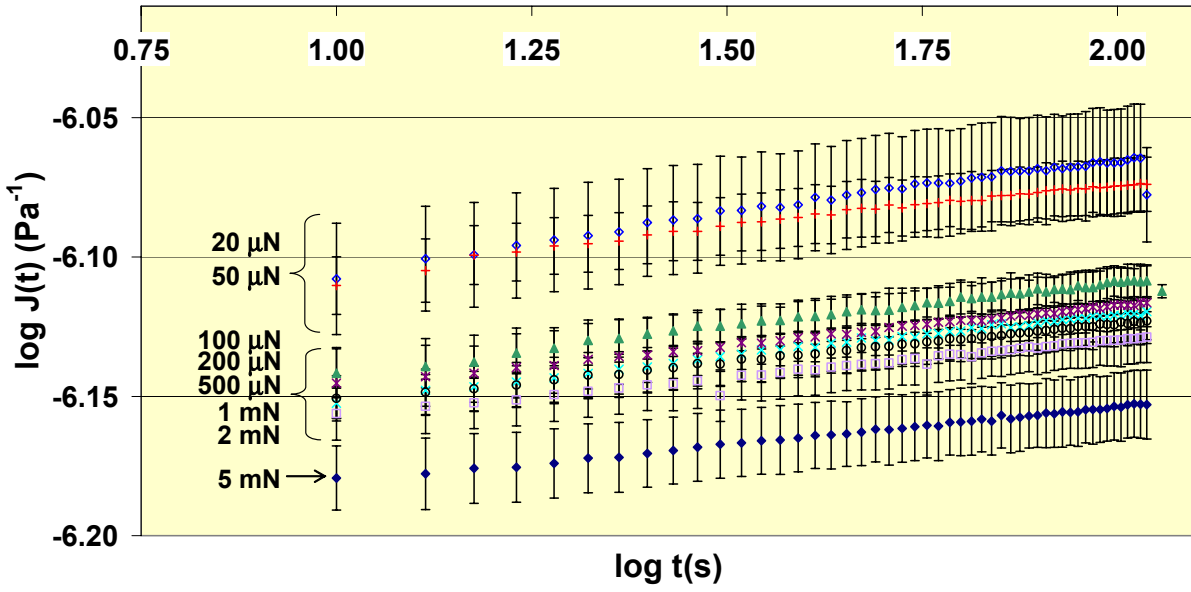
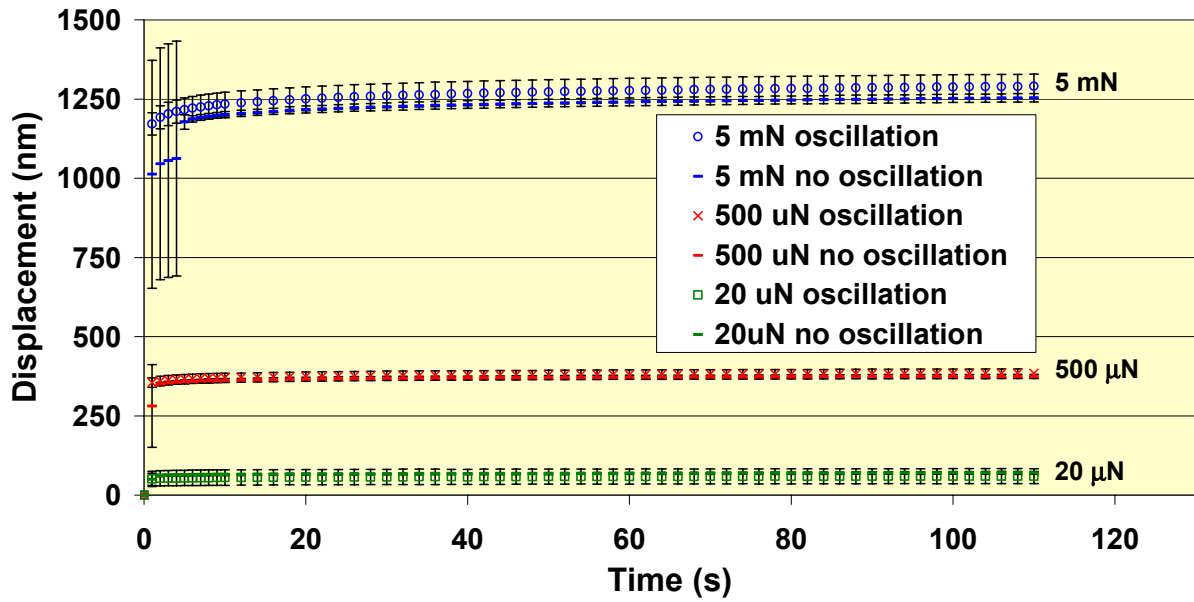
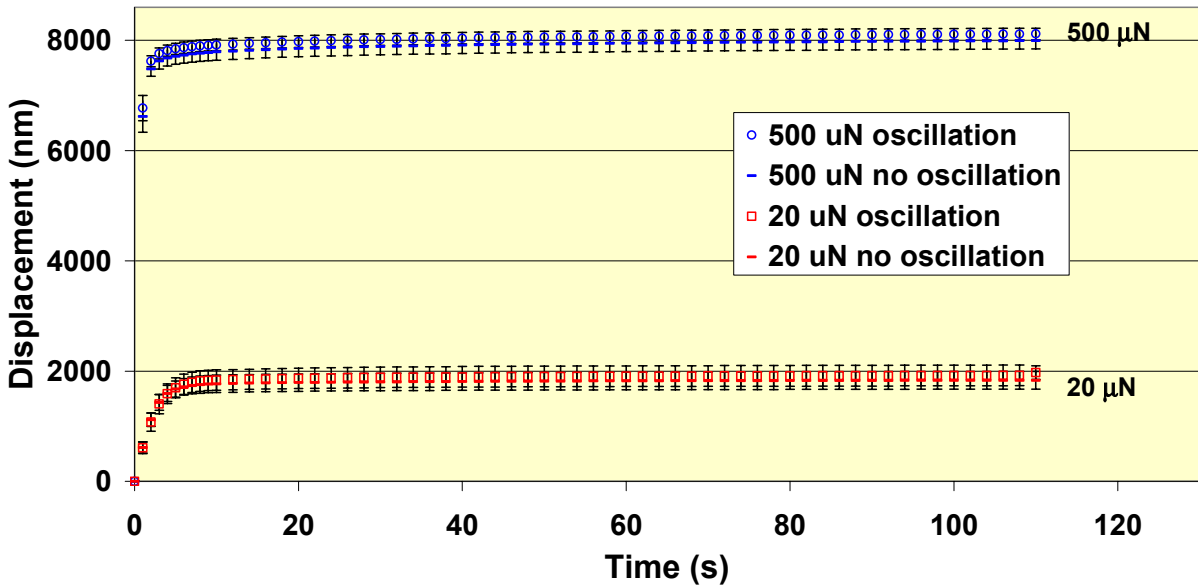


FIG. 8

VanLandingham et al.



(a)



(b)

FIG. 9

VanLandingham et al.

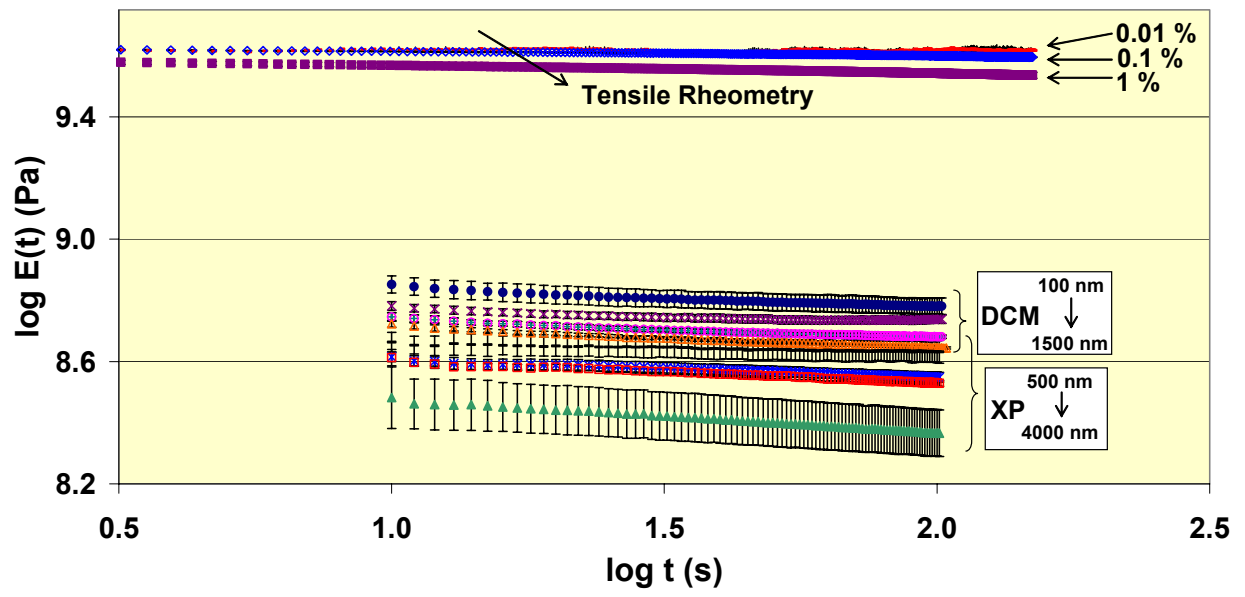


FIG. 10

VanLandingham et al.

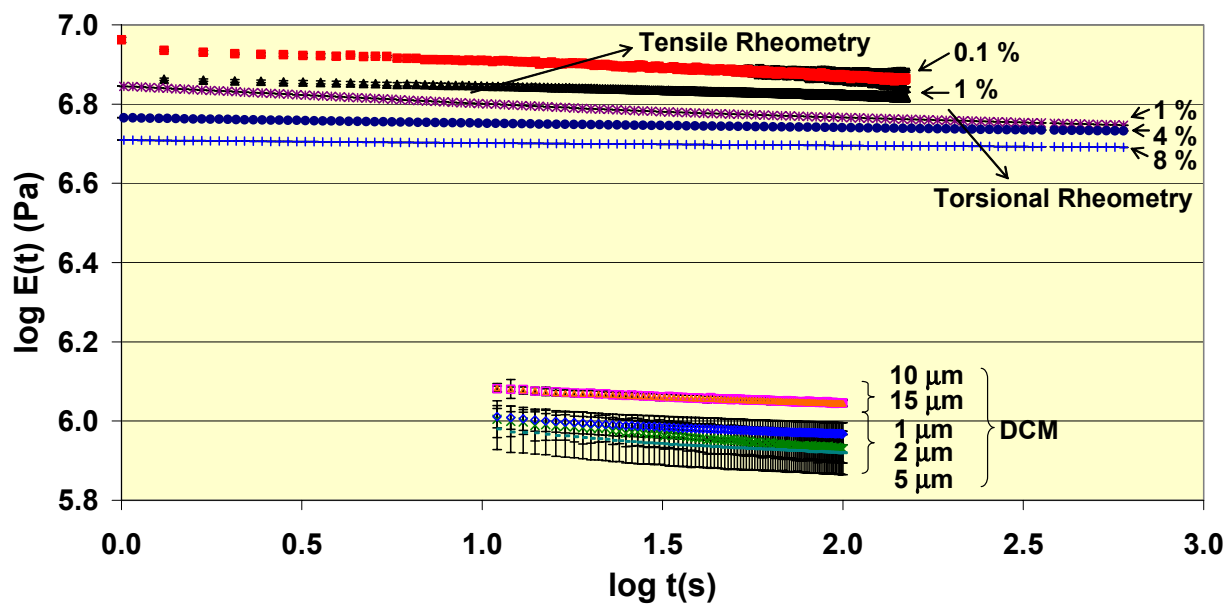


FIG. 11

VanLandingham et al.

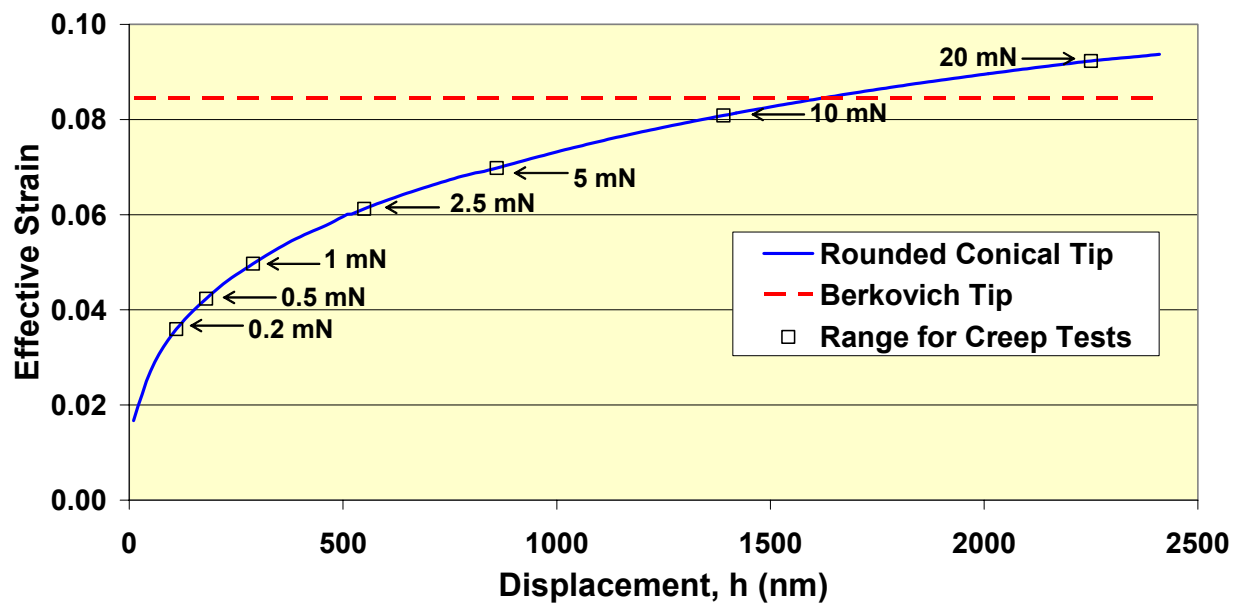


FIG. 12

VanLandingham et al.

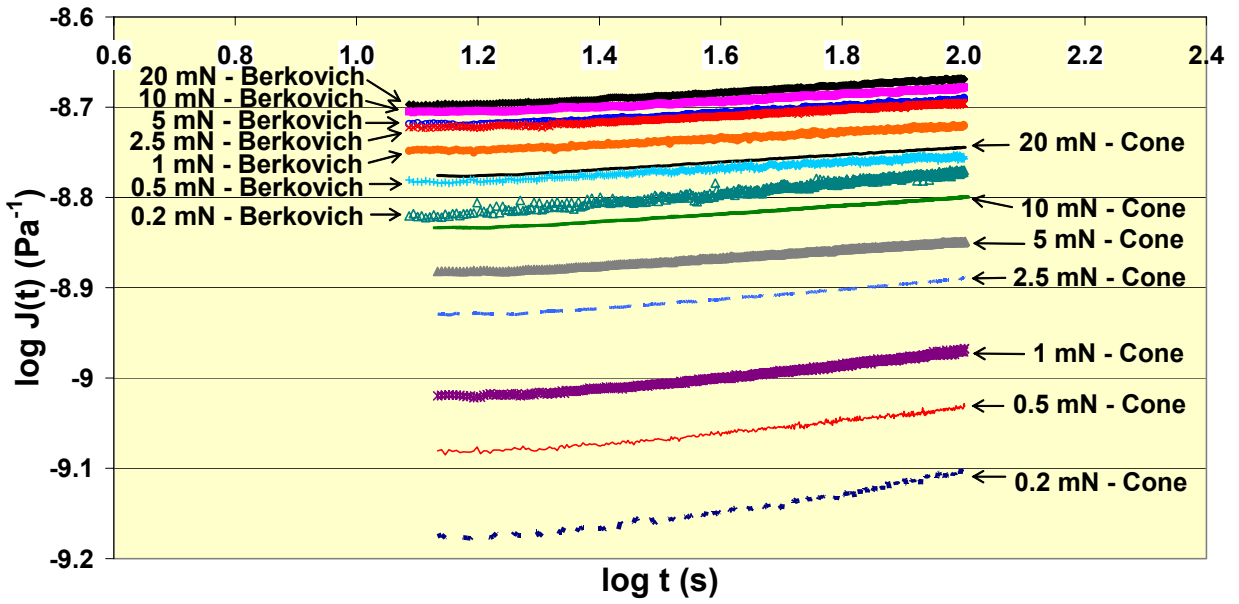


FIG. 13

VanLandingham et al.